HIGH EFFICIENCY LARGE AREA IBC SOLAR CELLS: PROCESSING AND CHARACTERIZATION

B.J. O'Sullivan[1]*, S. Singh[1], K. Manabu[2]. M Debucquoy[1], and J. Szlufcik[1]

[1] imec, Kapeldreef 75, Leuven, BELGIUM, [2] Kyocera Corporation, 1166-6 Hebimizo-cho, Shiga, JAPAN
* barry.osullivan@imec.be

ABSTRACT

Patterning techniques have been developed and applied to fabricate full-area interdigitated back contact solar cells on 156x156 mm^2 on n-Si wafers. The maximum efficiency obtained was 21.3%, enabled by V_{oc} values as high as 687 mV, but the cell performance was limited by a fill factor value of 77.4%. This was revealed to result from resistive losses emanating from the metal design, together with electrical shading from both emitter and BSF busbars, giving rise to lower FF and J_{sc} values.

1. INTRODUCTION

Interdigitated back contacted (IBC) silicon solar cells have been shown to achieve very high efficiencies, enabled by a structure with the terminals at the rear side, thereby allowing an efficient decoupling of the carrier generation at the front of the cell, and collection processes at the rear. Efficiencies as high as 25% have been reported for such cell structures on 125x125 mm^2 wafers [1], and 22.9% on 156x156 mm^2 [2]. However, despite the demonstrated high efficiencies, currently IBC processing on 156x156 mm^2 wafers is not industrialised, due to the complex processing involved in patterning, contacting and interconnecting two doped regions on the rear side.

The aim of this work is to report on our progress on IBC cells, fabricated on 156x156 mm^2 wafers. A high efficiency IBC cell process flow has been developed on 20x20 mm^2 solar cells, of which 25 were fabricated on a single 156x156 mm^2 Cz n-Si wafer. Initially, photolithography was used to pattern the diffused and contacted regions at the rear side of the cell [3]. Subsequently, efforts have been made to incorporate patterning methods that can be scaled up to fabricate large area cells, and to this end laser ablation together with screen printing have been employed on 20x20 mm^2 cells [4]. In this work, a process flow to fabricate solar cells employing the full area of a 156x156 mm^2 wafer is reported, comprising these laser and screen-printing based techniques.

2. PROCESS FLOW

In this work, these patterning techniques have been applied on a cell schematic, utilising the entire (semi-square) 156x156mm^2 surface. The challenge controlling the screen printed paste spreading, and resultant shunts,

imposed a design rule on the width of the metallised regions, with resultant fill factor loss [4].

After n-Si CZ wafer thinning, a BBr$_3$ diffusion is performed and the dopants are activated. On the wafer rear side, the BSF region is defined by ablating the oxide, prior to an emitter etch in these regions. Subsequently, the BSF diffusion and activation are performed, before the front side texturing process. This is followed by an FSF diffusion, and passivation by means of SiO$_2$/SiN$_x$. The regions to be contacted are defined by a further laser ablation step, prior to a blanket (3μm) Al-Si metallisation. The metal is etched, selectively by screen printing a polymer paste mask, before a final anneal step.

The solar cell has been re-designed, and differs from the two busbar design used for the small area cells to incorporate several rectangular unit cells connected in parallel. Electrical connections are made to numerous contact points along each busbar.

3. RESULTS

The light IV results are summarised in Table 1, and compared to the results from small area cells [4]. V_{oc} values are similar to those measured on small area cells (albeit on 156x156 mm^2 wafers), indicating the uniformity of the doping and passivation processes across the wafer surface. J_{sc} values are lower on the large cell, consistent with the presence of the busbars (notably BSF [5]) on the rear of the large area cells (not present for the small area cells). The best cell efficiency was 21.3%, and the fill factor measured at 77.4%, somewhat lower than the small cell performance. The pseudo fill factor values for both small and large cells are ~83.5%, indicating the potential of the cell design. The difference between FF and pFF indicates significant series resistance presence.

Table 1. Average and best results on 156x156 mm^2 IBC solar cells, measured under AM1.5 spectrum. Calibrated results obtained on small area cells [4] presented for comparison. Pseudo FF values measured from Suns-V_{oc} are also shown.

	Area [cm^2]	J_{sc} [mA/cm^2]	V_{oc} [mV]	FF [%]	pFF [%]	η [%]
Average (of 9)	239	40.2	685	76.5		21.0
Best cell	239	40.1	686	77.4	83.5	21.3
Best cell	4	41.3	687	78.5	83.6	22.2*

4. FILL FACTOR ANALYSIS

The mechanisms behind fill factor losses were examined further, using a combination of light IV, dark IV and Suns-V_{oc} measurements, on both large and small area cells. Measurements were performed on small area cells [4] using selective apertures to include none, one (BSF or emitter) or both busbars in the illuminated area, so their impact on device performance can be assessed, to elucidate the origin of losses observed.

In each case, the series, shunt, J_{02} losses were calculated as described in [6]. An additional busbar induced fill factor loss was incorporated, evaluated as highlighted in equation 1.

$$\Delta FF_{BB} = pFF - FF - \Delta FF_{R_s} \qquad (1)$$

The results are summarised in Figure 1, where it is clear that series resistance losses dominate the total fill factor loss for small and large area cells, independent on of aperture used, resulting in ~4 % (absolute) loss in fill factor. Losses originating from shunt or J_{02} are almost one order of magnitude lower. Resistive losses originating from the emitter busbar introduce an additional significant loss mechanism. Results on small area cells, with selective shading during measurement show that the FF loss arising from this can be as high as 3 % (absolute). When the BSF and emitter busbars are included in the measured area of the small cell, as shown in Figure 1, fill factor losses are similar to those of the large cell, whereby, series resistance and emitter busbar resistance losses dominate in both cases. Slight differences between small and large cells result from variations in busbar dimensions, and the metal thickness increase from 2 to 3 μm for large area cells.

There is of course a significant J_{sc} reduction resulting from the inclusion of the BSF busbar in the illuminated area, given absence of a junction under this region.
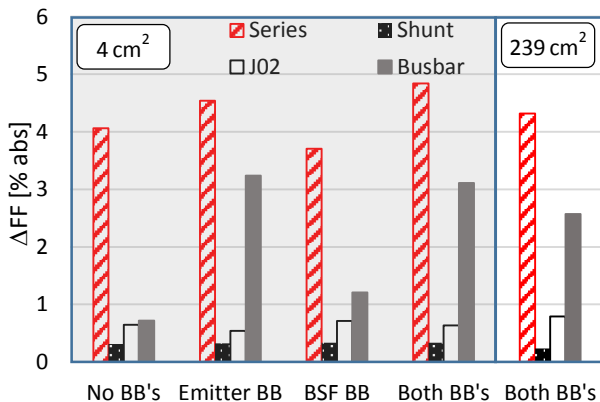

Figure 1. Decoupled fill factor losses for small and large area IBC cells, as a function of busbar(s) under illumination for small area cells. Specified busbars were illuminated using aperture masks, while the active area between busbars was always illuminated.

To ascertain the origin of the series resistance losses, electroluminescence was measured with a high resolution camera. The resultant image is shown in Figure 2, where the lateral non-uniformity in the region between the emitter and base busbars is clearly evident. That the highest response is detected adjacent to the BSF contact point is revealing, and points at resistance losses in the BSF busbar as being a significant loss mechanism.
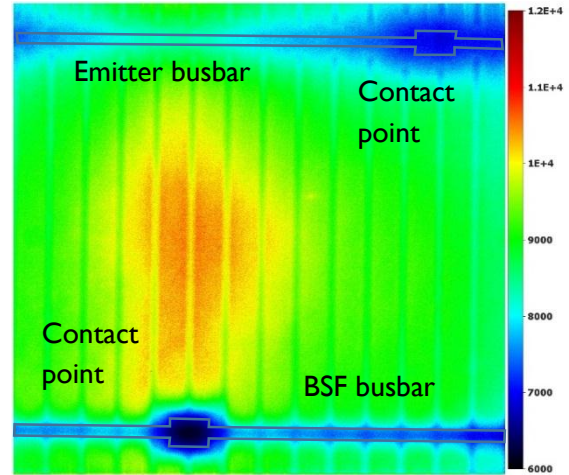

Figure 2. High resolution electroluminescence image of an IBC solar cell. The lateral non-uniformity of the response is clearly evident, as is the lower response from the busbars, and in particular contact points.

Given the aforementioned lateral non-uniformity, it is also concluded from this image that contact resistance is not the dominant mechanism in the series resistance losses, given that there are uniform pitches in contact holes, for both emitter and BSF regions, respectively, across the wafer. Clearly the process-induced design rules play a role in the resistive losses, with potential solutions including increasing the metal thickness, or the BB width. Given the results shown above, increasing the metal thickness is clearly the more promising route to pursue.

5. CONCLUSIONS

To conclude 156x156 mm^2 IBC solar cells have been fabricated on 156x156 mm^2 silicon wafers, where rear side patterning was performed by a combination of laser ablation and screen printing. Maximum efficiency of 21.3% was achieved, limited by fill factor losses induced by series and emitter busbar resistance, together with BSF busbar-induced J_{sc} loss.

6. REFERENCES

[1]   D Smith et al, *Proc. IEEE PVSC*, (2014)
[2]   Trina Solar, *press release*, (November 2014)
[3]   B O'Sullivan et al, *Proc. EU PVSEC* (2013), p956
[4]   S Singh et al, *Proc. EU PVSEC*, (2014), p672
[5]   M Hermle et al, Proc. *IEEE PVSC*, (2008)
[6]   A Khanna et al, *IEEE JPV*, **3**, (2013), p1170